JOURNAL OF APPLIED ELECTROCHEMISTRY 14 (1984) 305–314

Effect of acid and base additions on the corrosion behaviour of nickel in (Na,K)NO_3 melts

A. BARAKA, R. M. S. BARAKA

Chemistry Department, Faculty of Science, Cairo University, Cairo, Egypt

Received 28 April 1983; revised 15 June 1983

The effect of $NaPO_3$, NaH_2PO_4, Na_2HPO_4 and $K_2Cr_2O_7$ as acids and Na_2O_2, KOH and K_2CO_3 as bases on the corrosion behaviour of nickel in (Na, K)NO_3 melts has been examined at a temperature of 400° C. Weight-gain, potential-time and anodic polarization measurements were employed.

It was found that the acidic additions promote the corrosion of nickel and the extent of corrosion acceleration depends on the nature and concentration of the acid. The weight gain, the steady-state potential and the anodic polarization of nickel increase as a result of additions of these acids to the nitrate melt. The weight-gain measurements are noticeably higher when the amount of phosphate added to the melt is increased. On the other hand the presence of high concentrations of these additions decreases the steady-state potentials to less noble values. These acids intensify their attack at high concentration in the melt.

Na_2O_2, KOH and K_2CO_3, on the other hand, retard the corrosion at 400° C. Weight-gain, steady-state potentials and anodic polarization decrease upon addition of these bases. The nickel electrode behaves irreversibly in these melts. This may be attributed to the non-stoichiometry of NiO formed on the electrode surface.

1. Introduction

Potential/$_pO^{2-}$ diagrams for molten alkali nitrates [1, 2] predict an important role for the acidity (basicity) of the melt on the corrosion behaviour of the metals. Nickel undergoes corrosion in melts with low oxide ion content and passivates in basic melts. According to Lux [3], and Flood [4], acids and bases are defined as oxide-ion acceptors and donors respectively and the function

$$_pO^{2-} = -\log[O^{2-}] \quad (1)$$

has been taken as a measure of the acidity (basicity) of an oxyanionic melt. A high value of $_pO^{2-}$ characterizes an acidic melt, whilst a low value characterizes a basic one.

The kinetics of the oxidation of nickel in (Na, K)NO_3 melts using gravimetric, open circuit potential and anodic polarization measurements have been reported [5]. The results were interpreted in relation to available data on the kinetics of oxidation of nickel in nitrate melts and in air at high temperatures.

In this work the effect of $NaPO_3$, NaH_2PO_4, Na_2HPO_4 and $K_2Cr_2O_7$ as acids and Na_2O_2, KOH and K_2CO_3 as bases on the corrosion behaviour of nickel in (Na, K)NO_3 melts has been investigated at a temperature of 400° C. Weight-change, open circuit potential and galvanostatic anodic polarization measurements were employed.

2. Experimental details

The $NaNO_3$–KNO_3 eutectic (50:50/mol:mol; m.p. 225° C) was prepared and dried as previously described [5, 6], the calculated amounts of the two salts (AR, Merck, Germany) being mixed together and melted at 350° C. The last traces of water were removed by bubbling pure, dry oxygen gas through the melt for a period of two hours. Excess oxygen was then removed by bubbling pure and dry nitrogen for about 30 min. The eutectic thus prepared was left to cool in a dry atmosphere and the solidified mass was quickly crushed and kept in a closed dessicator until required. In each experiment 100.0 g of the melt was used, and this was melted at the working temperature.

Experiments were carried out in tall unlipped

0021–891X/84 $03.00 + .12

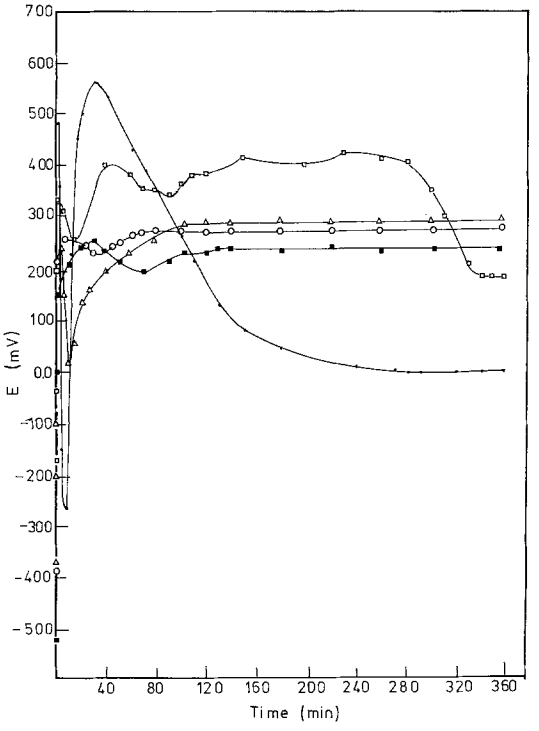

Fig. 1. Potential–time curves of nickel in (Na, K)NO_3 in the presence of different molal concentrations of $NaPO_3$ at 400° C. ▪ 0.02 mol dm^{-3}, ○ 0.05 mol dm^{-3}, △ 0.10 mol dm^{-3}, □ 0.20 mol dm^{-3}, • 0.50 mol dm^{-3}.

Pyrex glass tubes (5 cm diameter × 11 cm length). The attack on glass by the melt was negligible and the containers were usable for a large number of experiments. The working vessel was surrounded by an aluminium container (7 cm diameter × 10 cm length) which was placed in an electrically heated crucible-type furnace. Regulation of temperature was effected through a variable transformer. The temperature was measured by means of a Ni/Ni–Cr thermocouple and a temperature indicator (± 2° C). The thermocouple was separated from the melt by a tight-fitting Pyrex glass tube. The electrodes were cut from nickel sheet (BDH, England) 1 mm thick. The electrodes, 0.5 × 0.5 cm^2, had a side-arm, 20 × 0.1 cm^2, for electrical connection. The auxiliary electrode of platinum sheet, 1 × 1 cm^2, was sealed to a platinum wire and contained in a Pyrex glass tube with a medium porosity glass-frit disc sealed at the bottom end. A fresh electrode was used in each experiment. Just before introduction to the melt, the electrode was abraded with 2/0 emery paper and degreased with ether. Then the nickel electrode was introduced into the melt and left until the steady-state potential was established. A small anodic current was then imposed and the corresponding potential was measured after 5 min of polarization. The current was then disconnected for 5 min. After this the anodic polarization was again started with a higher current density. The process of connecting and disconnecting of the current was repeated to the end of the experiment. The potential of the test electrode was measured relative to an Ag/Ag(I), melt/glass reference electrode [5, 6], using a Pye Unicam Potentiometer. A 99.9+% pure silver wire was dipped in $NaNO_3$–KNO_3 eutectic containing 2.04 wt % $AgNO_3$. The reference half cell was separated from the main melt by a solid Pyrex-glass tubing. This possessed sufficient electrical conductance at these high temperatures to permit definite potential to be measured.

For the weight-change experiments, specimens, 2 × 1 cm, were used. These were supported in the melt by a glass hook passing through a small hole near the upper edge of the sheet.

3. Results

3.1. *Open circuit potential measurements*

Potential/time curves for the nickel electrode in $NaNO_3$–KNO_3 eutectic made acidic with $NaPO_3$, NaH_2PO_4, Na_2HPO_4 or $K_2Cr_2O_7$ and basic with Na_2O_2, KOH or K_2CO_3 are given in Figs. 1–7 at a temperature of 400° C. These results show generally that the potential of the nickel electrode changes with time towards more positive (nobler) values. Steady-state potentials were attained after limited reaction times, depending on the type and concentration of the additive. Inspection of these curves reveals that in the case of acid additives the potential was found to fluctuate before attaining the steady-values. In the case of $K_2Cr_2O_7$ less fluctuations were recorded. In the case of basic additives no fluctuations in the potential were observed.

The variation of the steady-state potential with the logarithm of the molal concentration of the acidic and basic additives is shown respectively by the curves of Figs. 8 and 9. These results indicate that the relation between the two variables gives continuous and discontinuous straight lines in the case of basic and acidic additives respectively.

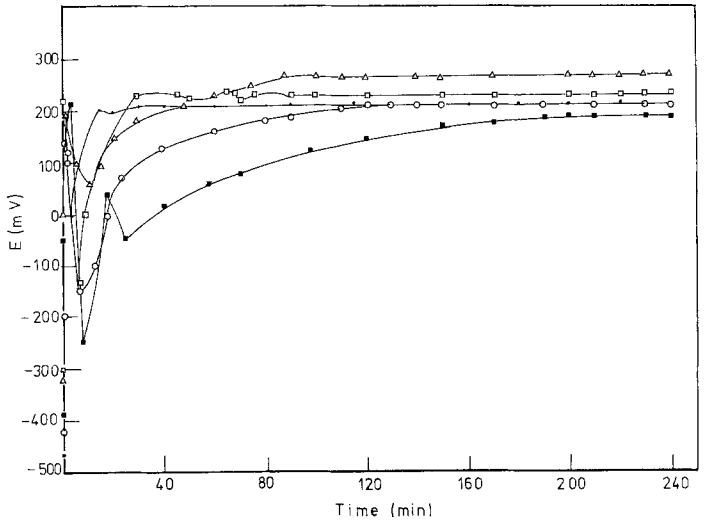

Fig. 2. Potential–time curves of nickel in (Na, K)NO_3 in the presence of different molal concentrations of NaH_2PO_4 at 400° C. ■ 0.02 mol dm^{-3}, ○ 0.05 mol dm^{-3}, △ 0.10 mol dm^{-3}, □ 0.20 mol dm^{-3}, ● 0.50 mol dm^{-3}.

In the case of acidic additives $NaPO_3$, NaH_2PO_4, Na_2HPO_4 and $K_2Cr_2O_7$ the presence of small concentrations (up to 0.1 mol dm^{-3}) was accompanied by an ennoblement (positivation) of the steady-state potential. The addition of high concentrations of these additives in the melt brings about an opposite effect i.e. the steady-state potential decreases (to less positive values). The rate at which the steady-state potential varies with $\log C$ depends on the nature of the acid used (see Fig. 8).

On the other hand, the steady-state potential attained for the nickel electrode in basic melts decreases (to more negative values) as the concentration of the base added increases (see Fig. 9). The steady-state potential was found to decrease with the concentration of Na_2O_2 and KOH at a higher rate than in the case of K_2CO_3.

3.2. *Weight gain measurements*

The effect of increasing additions of acids $NaPO_3$, NaH_2PO_4, Na_2HPO_4 and $K_2Cr_2O_7$ and bases Na_2O_2, KOH and K_2CO_3 on the corrosion rate of nickel in (Na, K)NO_3 melt at a temperature of 400° C is shown respectively in Figs. 10 and 11. These plots represent the variation of the weight gain of nickel specimens with the logarithm of the molal concentration of the additives. In all experiments the weight gain of the specimens was measured after a reaction time of 8 h.

As is seen from the results of Fig. 10, the acidic

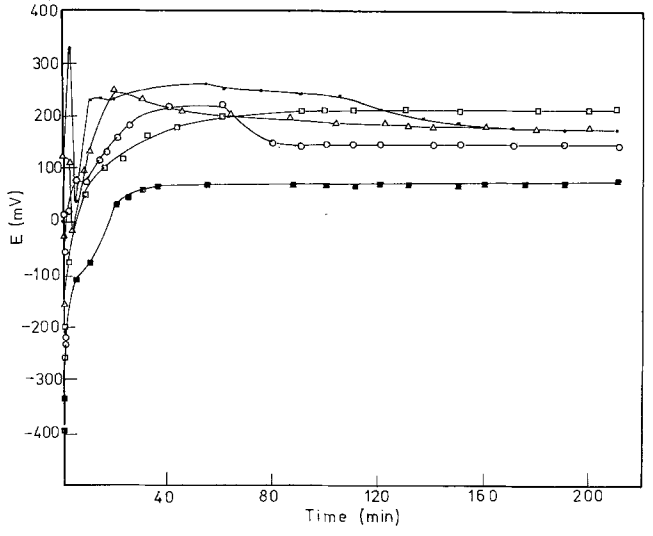

Fig. 3. Potential–time curves on nickel in (Na, K)NO_3 in the presence of different molal concentrations of Na_2HPO_4 at 400° C. ■ 0.02 mol dm^{-3}, ○ 0.05 mol dm^{-3}, △ 0.10 mol dm^{-3}, □ 0.20 mol dm^{-3}, ● 0.50 mol dm^{-3}.

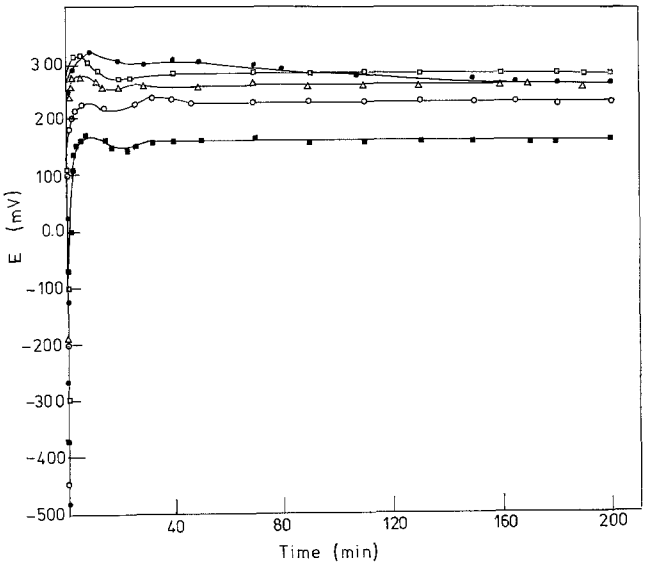

Fig. 4. Potential–time curves of nickel in (Na, K)NO_3 in the presence of different molal concentrations of $K_2Cr_2O_7$ at 400° C. ■ 0.02 mol dm^{-3}, ○ 0.05 mol dm^{-3}, △ 0.10 mol dm^{-3}, □ 0.20 mol dm^{-3}, ● 0.50 mol dm^{-3}.

additives promote the corrosion of nickel, and the extent of corrosion acceleration depends on the nature and concentration of the acid in the melt. The weight gain in the presence of $NaPO_3$, NaH_2PO_4 and Na_2HPO_4 varies at a higher rate than the corresponding gain in the presence of $K_2Cr_2O_7$.

The plots (lines) of Fig. 11 show the retarding effect of the bases Na_2O_2, KOH and K_2CO_3 on the corrosion of nickel in the nitrate melt at a temperature of 400° C. The increase of base concentration was accompanied by a decrease in the weight gain.

Within the concentration range studied the vari-

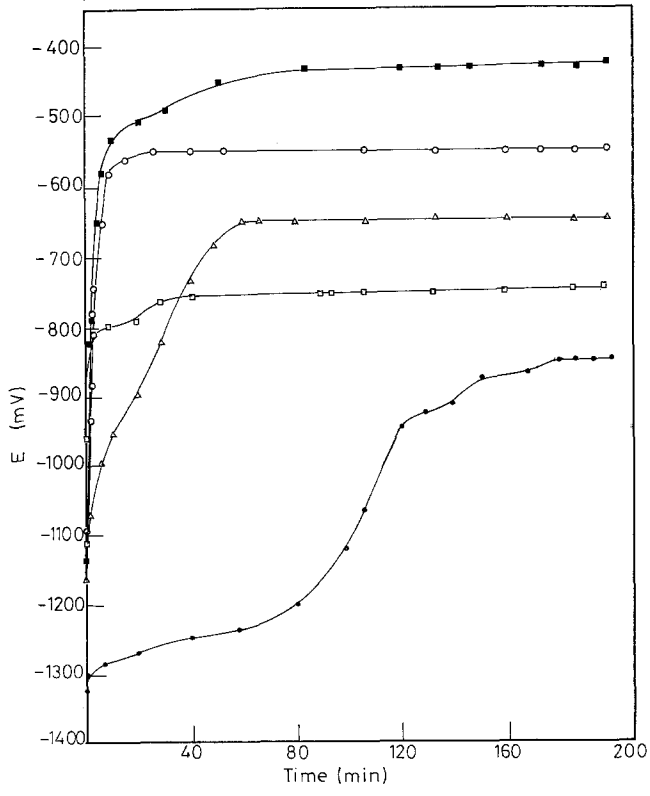

Fig. 5. Potential–time curves of nickel in (Na, K)NO_3 in the presence of different molal concentrations of Na_2O_2 at 400° C. ■ 0.02 mol dm^{-3}, ○ 0.05 mol dm^{-3}, △ 0.10 mol dm^{-3}, □ 0.20 mol dm^{-3}, ● 0.50 mol dm^{-3}.

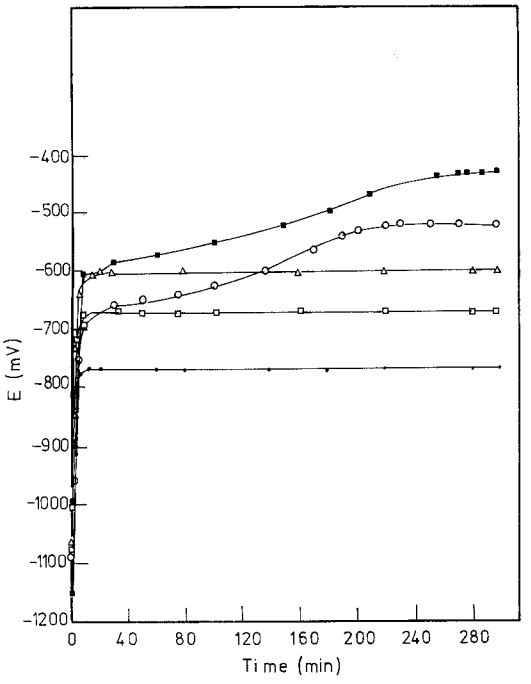

Fig. 6. Potential–time curves of nickel in (Na, K)NO_3 in the presence of the different molal concentrations of KOH at 400° C. ■ 0.02 mol dm^{-3}, ○ 0.05 mol dm^{-3}, △ 0.10 mol dm^{-3}, □ 0.20 mol dm^{-3}, ● 0.50 mol dm^{-3}.

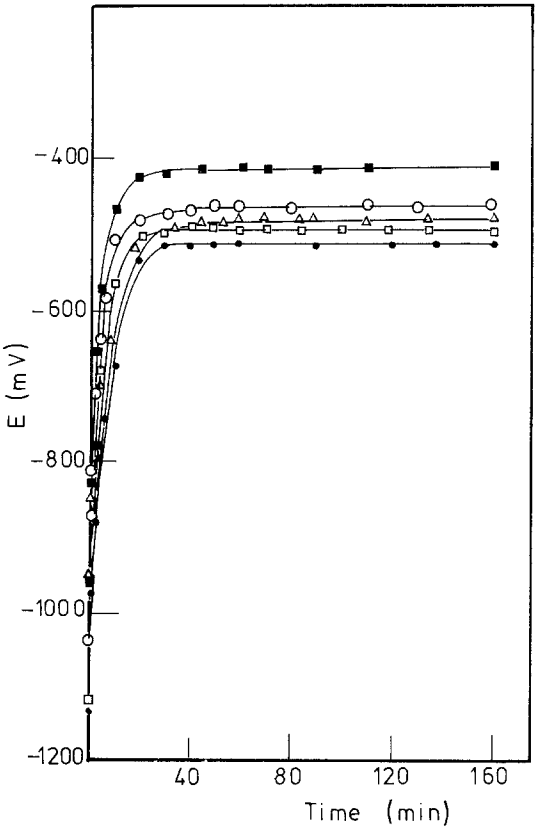

Fig. 7. Potential–time curves of nickel in (Na, K)NO_3 in the presence of different molal concentrations of K_2CO_3 at 400° C. ■ 0.02 mol dm^{-3}, ○ 0.05 mol dm^{-3}, △ 0.10 mol dm^{-3}, □ 0.20 mol dm^{-3}, ● 0.50 mol dm^{-3}.

ation of the corrosion rate of nickel in the nitrate eutectic with the concentration of the examined additives could be represented in most cases by the linear relation:

$$\omega = a \pm b \log C \qquad (2)$$

where a and b are constants depending on the nature of the additives.

3.3. *Anodic polarization*

Semilogarithmic plots of galvanostatic oxidation for a nickel electrode in $NaNO_3$–KNO_3 eutectic, made acidic with $NaPO_3$ or $K_2Cr_2O_7$ and basic with Na_2O_2 or KOH at 400° C, are shown in Figs. 12 and 13. These results show clearly that the anodic polarization of the nickel electrode increases in the presence of acidic additives and decreases in basic melts.

In the presence of the acidic additives $NaPO_3$ and $K_2Cr_2O_7$, an increase of the acid concentration was accompanied by an increase in the degree of anodic polarization of the nickel electrode.

In basic melts the anodic polarization of the nickel electrode decreases with increasing concentration of the base added.

4. Discussion

4.1. *Acidic melts*

According to the views of Duke and his co-workers [7–11], the equilibrium:

$$NO_3^- \rightleftharpoons NO_2^+ + O^{2-} \qquad (3)$$

is attained in molten nitrates, whose equilibrium constant at various tempteratures is known [12].

The addition of an acid (O^{2-} ion-acceptor) to the melt should shift this equilibrium towards more nitryl ion, NO_2^+, formation to an extent depending on the strength of the acid added. The concentration of NO_2^+ ion in the melt is, therefore, a measure of the acidity of the added anion.

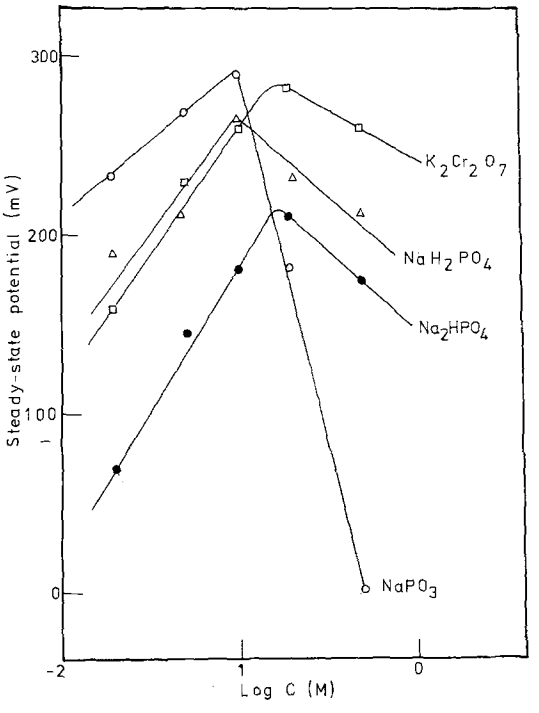

Fig. 8. Variation of steady-state potential of nickel electrode with log C of $NaPO_3$, NaH_2PO_4, Na_2HPO_4 and $K_2Cr_2O_7$.

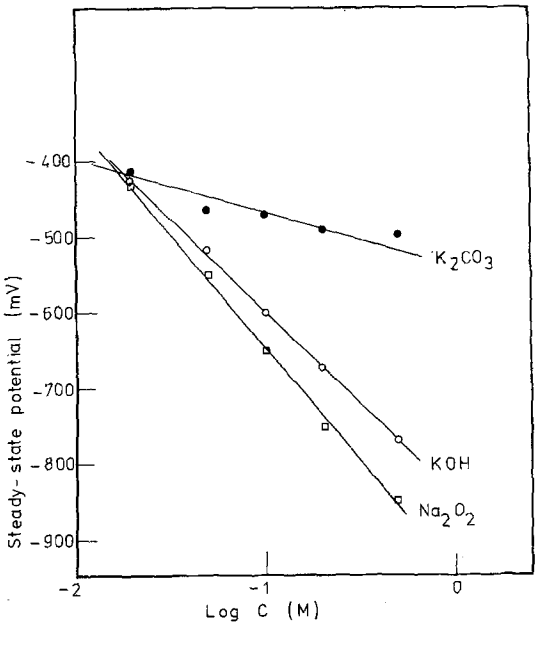

Fig. 9. Variation of steady-state potential of nickel electrode with log C of Na_2O_2, KOH and K_2CO_3 at 400° C.

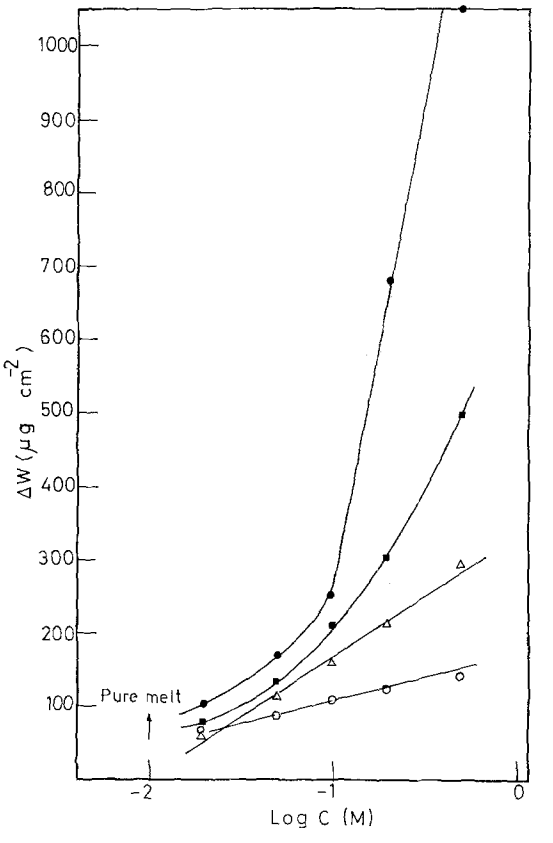

Fig. 10. Variation of weight gain of nickel after 8 h in (Na, K)NO_3 melt with log C of acid additives at 400° C. • $NaPO_3$, □ NaH_2PO_4, △ K_2HPO_4, ○ $K_2Cr_2O_7$.

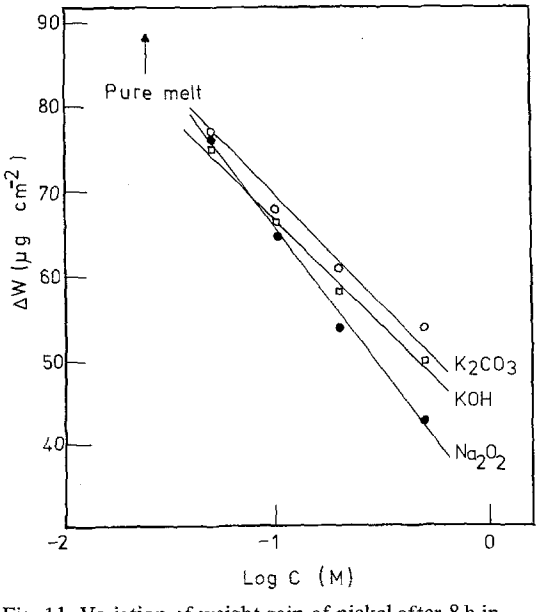

Fig. 11. Variation of weight gain of nickel after 8 h in (Na, K)NO_3 melt log C of base additives at 400° C.

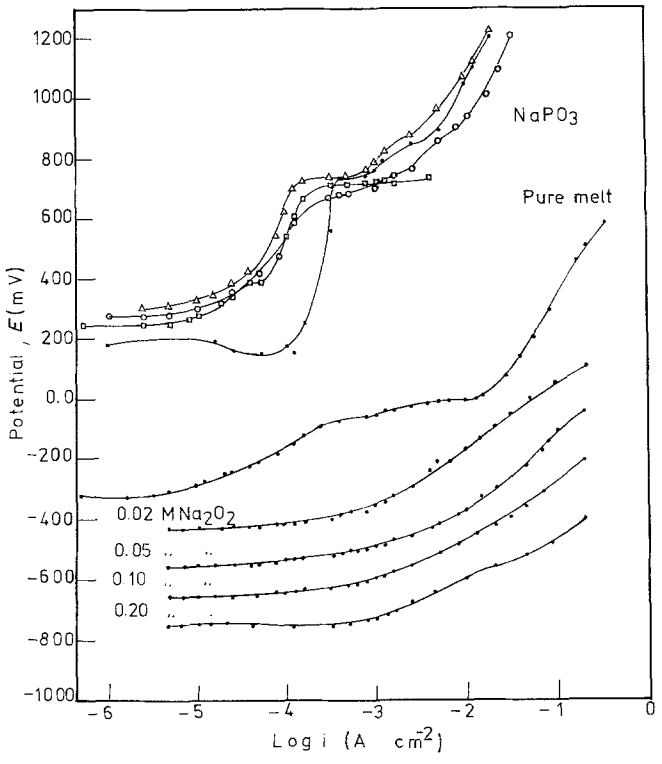

Fig. 12. Semilogarithmic plots of galvanostatic oxidation of nickel in (Na, K)NO_3 melt at 400° C in the presence of $NaPO_3$ or Na_2O_2. □ 0.02 mol dm^{-3}, ○ 0.05 mol dm^{-3}, △ 0.10 mol dm^{-3}, • 0.20 mol dm^{-3}.

The constant of equilibrium for Equation 3 can be expressed as

$$K_1 = [NO_2^+][O^{2-}] \qquad (4)$$

Assuming $[NO_3^+] = 1$ and substituting for $[O^{2-}]$ in the Nernst equation for the nickel electrode in molten nitrates [1]

$$E = E^0 - \frac{RT}{2F}\ln[O^{2-}] \qquad (5)$$

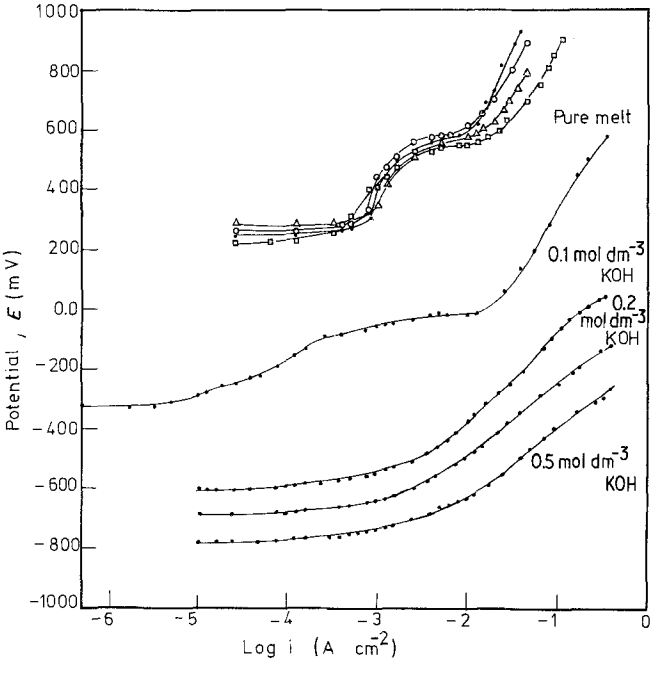

Fig. 13. Semilogarithmic plots of galvanostatic oxidation of nickel in (Na, K)NO_3 melt at 400° C in the presence of $K_2Cr_2O_7$ or KOH. □ 0.05 mol dm^{-3} $K_2Cr_2O_7$, ○ 0.10 mol dm^{-3} $K_2Cr_2O_7$, △ 0.20 mol dm^{-3} $K_2Cr_2O_7$, • 0.50 mol dm^{-3} $K_2Cr_2O_7$.

we get

$$E = E^0 - \frac{RT}{2F}\ln K_1 + \frac{RT}{2F}\ln[NO_2^+] \quad (6)$$

The reaction of the acids $NaPO_3$, NaH_2PO_4, Na_2HPO_4 and $K_2Cr_2O_7$ with the nitrate melt can be expressed by the following equilibria

$$2PO_3^- + NO_3^- \rightleftharpoons P_2O_7^{4-} + NO_2^+ \quad (7)$$

$$2H_2PO_4^- + NO_3^- \rightleftharpoons 2HPO_4^{2-} + H_2O + NO_2^+ \quad (8)$$

$$2HPO_4^{2-} + NO_3^- \rightleftharpoons 2PO_4^{3-} + H_2O + NO_2^+ \quad (9)$$

and

$$Cr_2O_7^{2-} + NO_3^- \rightleftharpoons 2CrO_4^{2-} + NO_2^+ \quad (10)$$

Assuming that $[NO_3^-] = 1$, the equilibria constants of Reactions 7–10 are

$$K_7 = \frac{[P_2O_7^{4-}]}{[PO_3^-]^2}[NO_2^+] \quad (11)$$

$$K_8 = \frac{[HPO_4^{2-}]^2[H_2O]}{[H_2PO_4^-]^2}[NO_2^+] \quad (12)$$

$$K_9 = \frac{[PO_4^{3-}]^2[H_2O]}{[HPO_4^{2-}]^2}[NO_2^+] \quad (13)$$

$$K_{10} = \frac{[CrO_4^{2-}]^2}{[Cr_2O_7^{2-}]}[NO_2^+] \quad (14)$$

Substituting for the value of $[NO_2^+]$ in Equation 6, an expression for the electrode potential in the presence of $NaPO_3$ is given as

$$E = E^0 - \frac{RT}{2F}\ln K_1 + \frac{RT}{2F}\ln K_4 + \frac{RT}{2F}\ln\frac{[PO_3^-]^2}{[P_2O_7^{4-}]}$$

$$= E_1^0 + \frac{RT}{2F}\ln\frac{[PO_3^-]^2}{[P_2O_7^{4-}]} \quad (15)$$

in the presence of NaH_2PO_4 we get

$$E = E_2^0 + \frac{RT}{2F}\ln\frac{[H_2PO_4^-]^2}{[HPO_4^{2-}][H_2O]} \quad (16)$$

in the presence of Na_2HPO_4 we get

$$E = E_3^0 + \frac{RT}{2F}\ln\frac{[HPO_4^{2-}]^2}{[PO_4^{3-}]^2[H_2O]} \quad (17)$$

Similarly in the presence of $K_2Cr_2O_7$ we get

$$E = E_4^0 + \frac{RT}{2F}\ln\frac{[Cr_2O_7^{2-}]}{[CrO_4^{2-}]^2} \quad (18)$$

Equations 15–18 indicate that the potential of the nickel electrode should vary with the concentration of the added acid in a positive direction (more noble values), at a rate depending upon the strength of the acid. The results of Figs. 1–4, 8 are in agreement with these predictions.

Previous publications [13–15], as well as the results of the present study [5] show that nickel oxidizes in the nitrite or nitrate melt into mainly NiO. It can be suggested here that the oxidation of nickel takes place in the following steps:

The anodic reaction:

$$Ni \rightleftharpoons Ni^{2+} + 2e^-$$

in the presence of the equilibrium:

$$NO_3^- \rightleftharpoons NO_2^+ + O^{2-}$$

followed by:

$$Ni^{2+} + O^{2-} \rightleftharpoons NiO$$

and the cathodic reaction is:

$$NO_2^+ + e^- \rightleftharpoons NO_2$$

In the presence of acidic additives, the concentration of O^{2-} ion decreases and that of NO_2^+ increases. In accordance with this suggestion, the two effects would promote the corrosion attack of the metal to an extent depending upon the acidity of the melt. The results of Fig. 10 confirm the above predictions. These findings are in agreement with those previously obtained by Brough and Kerridge [16] from their investigation of the reactions of different metals with (Li, K)NO_3 eutectic. With less strongly reducing metals, such as iron and nickel, more nitrogen dioxide was evolved when the melt was acidified with pyrosulphate or dichromate. They have suggested that nitrogen dioxide was produced by a process involving electron transfer to the nitryl ion i.e.

$$M + NO_2^+ \longrightarrow M^+ + NO_2 \quad (19)$$

This reaction may facilitate the formation of other insoluble products on the metal surface, rather than metal oxide.

The presence of phosphate additions in the melt gives abnormally high weight gain results in comparison with those in the case of $K_2Cr_2O_7$. This effect is very clear, especially, at high concentrations of phosphate additions, Fig. 10. The presence of phosphate in the melt may enhance the formation of a thick layer of insoluble nickel phosphate on the nickel specimens. The attack of

the added phosphates may be intensified at high concentrations. This may give rise to the abnormally very high weight gain which corresponds to the increased gradient of the curves in Fig. 10 for phosphates.

The decrease of the steady-state potential observed in the presence of high concentrations of the acidic additives, Fig. 8 may be explained as follows. The presence of the acid in the nitrate melt shifts the equilibrium $NO_3^- \rightleftharpoons NO_2^+ + O^{2-}$ to the right giving rise to the formation of excess amounts of nitryl ions (NO_2^+). These ions have relatively strong oxidizing properties and can react with the metal according to the reaction [16].

$$M + NO_2^+ \longrightarrow M^+ + NO_2 \qquad (20)$$

This attack may be intensified at high concentrations of the acidic additive. Also this reaction may enhance the formation of products other than an oxide layer, especially in the presence of phosphate additions. The nickel metal is very sensitive to the oxidizing agents (ions), such as NO_2^+, the presence of which causes an attack on the nickel. The addition of increasing amounts of acidic additives to the nitrate melt increases the activity of these nitryl ions to a large extent which can intensify their attack on nickel by Reaction 20. These effects may decrease the steady-state of the electrode potential (to less noble values) at the high concentrations of acid additions, depending on the nature of the acid added. These results are qualitatively in agreement with those obtained from the weight gain measurements.

4.2. *Basic melts*

In accordance with the above hypothesis and with the thermodynamic predictions of nickel in molten alkali nitrates [1], basic melts, on the other hand, should enhance the passivity of the metal. The results obtained at a temperature of 400° C are in good agreement with these views. The corrosion rate was found to decrease as the oxide ion content of the melt increased by the addition of Na_2O_2, KOH and K_2CO_3 to the melt (see Fig. 11).

The passivated metal in these melts would function as a metal/metal oxide electrode, and its potential should vary with the oxide ion concentration according to the Nernst equation [1]

$$E = E^0 - \frac{RT}{2F} \ln[O^{2-}] \qquad (5)$$

The potential decreases to less noble values as the concentration of oxide ions increases by a basic additive.

The results of Fig. 9 confirm this relation. The potential of the nickel electrode varied linearly with the logarithm of the oxide ion concentration. The slopes of the plots are 333, 250 and 85 mV for Na_2O_2, KOH and K_2CO_3 respectively. These values are larger than the expected slope $RT/2F$ (67 mV). This means that this electrode behaves irreversibly in these melts. This type of irreversible behaviour of the nickel electrode in these melts has been reported by Laitinen *et al.* [17] who explained it on the basis of the formation of higher oxides. This irreversible behaviour may be attributed to the nonstoichiometry of NiO. Also this type of irreversible behaviour is observed for alkali nitrate melt, and has been reported in the literature for the oxygen electrode [18–24].

The passivating film consisting mainly of NiO is formed according to the following reaction

$$Ni + O^{2-} \rightleftharpoons NiO + 2e^- \qquad (21)$$

The Nernst equation for Reaction 21 is

$$E = E^0 + \frac{2.303RT}{2F} {}_pO^{2-} \qquad (22)$$

The change of potential at constant temperature should, therefore, be dependent on the oxide ion concentration.

These thermodynamic calculations for the nickel electrode in molten alkali nitrates [1] assist in the elucidation of the possible reaction processes involved within the different potential regions. Thus the following equilibria with their Nernst equations calculated at 600 K [1], appear to be of value for the interpretation of the present results.

$$Ni + O^{2-} \rightleftharpoons NiO + 2e^- \qquad (21)$$

$$E = -2.736 + 0.0595\,{}_pO^{2-}$$

$$O^{2-} \rightleftharpoons \tfrac{1}{2}O_2 + 2e^- \qquad (23)$$

$$E = -1.758 + 0.298 \log[PO_2] + 0.0595\,{}_pO^{2-}$$

Equations 21 and 23 indicate that the potential of the nickel electrode should become more positive with an increase in acid concentration, at a rate

depending on the strength of the acid, and also that the potential of the nickel electrode should become more negative with increasing concentration of added base. The results in Figs. 12 and 13 agree with these predictions.

The results obtained in these measurements, combined with the constant in the following equations based on the theory of absolute reaction rates permit a closer examination of this electrode reaction

i. Consider the case where Reaction 21 is the rate determining step, hence the velocity of this reaction is

$$V_{13} = K_{13}[O^{2-}]\, e^{(2\beta\eta F/RT)} \qquad (24)$$

The rate equation expressing the current density (i) is derived in the conventional manner [25, 26]. The derivation yields

$$i = 2FK_{13}[O^{2-}]\, e^{(2\beta\eta F/RT)} \qquad (25)$$

where K_{13} is a general constant for combined rate and equilibrium contstant, β is the symmetry factor, R is the gas constant, F is the Faraday number and η is the anodic polarization. Taking the logarithm of Equation 25 and rearranging gives

$$\eta = a \log 2FK_{13} - a_p O^{2-} - a \log i \qquad (26)$$

where $a = -2.303RT/2\beta F$

ii. Consider the case where Reaction 23 is the rate determining step, hence the velocity of the reaction is

$$V_{14} = K_{14}[O^{2-}]({}_pO_2)^{-1/2} \cdot e^{2\beta\eta F/RT} \qquad (27)$$

In atmospheric conditions (${}_pO_2 = 0.2$) this equation becomes

$$V_{14} = K_{14}^{-}[O^{2-}]\, e^{2\beta\eta F/RT} \qquad (28)$$

The rate equation expressing the current density (i) is

$$i = 2FK_{14}^{-}[O^{2-}]\, e^{2\beta\eta F/RT} \qquad (29)$$

Taking the logarithm of Equation 29 and rearranging gives

$$\eta = a \log 2FK_{14}^{-} - a_p O^{2-} - a \log i \qquad (30)$$

where $a = -2.303RT/2\beta F$.

It is clear from Equations 29 and 30, that at constant current density, there is a linear relationship between η and ${}_pO^{2-}$. This indicates that the anodic polarization of the nickel electrode should increase in acidic melts and decreases in basic ones. The results of Figs. 12 and 13 are in agreement with this prediction.

References

[1] S. I. Marchiano and A. J. Arvia, *Electrochim. Acta* **17** (1972) 861.
[2] A. Conte and S. Casadio, *Ric Sci* **36** (1966) 433.
[3] H. Lux, *Z. Electrochem.* **45** (1939) 303.
[4] H. Flood and T. Förland, *Acta Chem. Scand.* **1** (1947) 592.
[5] R. M. S. Baraka, MSc Thesis, Cairo University (1983).
[6] A. M. Shams El-Din, A. A. El-Hosary and A. A. A. Gerges, *J. Electroanal. Chem.* **6** (1963) 131.
[7] F. R. Duke and X. X. Yamamoto, *J. Amer. Chem. Soc.* **81** (1959) 6378.
[8] F. R. Duke and M. L. Iverson, *ibid.* **80** (1958) 5061.
[9] F. R. Duke and J. Schlegel, *J. Phys. Chem.* **67** (1963) 2487.
[10] F. R. Duke and M. L. Iverson, *Anal. Chem.* **31** (1959) 1233
[11] R. N. Kust and F. R. Duke, *J. Amer. Chem. Soc.* **85** (1963) 3338.
[12] R. N. Kust, *J. Electrochem. Soc.* **116** (1969) 1137.
[13] A. J. Arvia, J. J. Podesta and R. C. V. Piatti, *Electrochim. Acta* **16** (1971) 1979.
[14] *Idem, ibid.* **17** (1972) 889.
[15] *Idem, ibid.* **17** (1972) 901.
[16] B. J. Brough and D. H. Kerridge, *Inorg. Chem.* **4** (1965) 1353.
[17] H. A. Laitnen and B. B. Bhatia, *J. Electrochem. Soc.* **107** (1960) 705.
[18] R. G. Zambonin and J. Jordan, *J. Amer. Chem. Soc.* **89** (1967) 6365.
[19] *Idem, ibid.* **91** (1969) 2225.
[20] N. S. Wrench and D. Inman, *J. Electroanal. Chem.* **7** (1968) 319.
[21] R. G. Zambonin, *ibid.* **24** (1970) 25.
[22] J. Jordan, *ibid.* **29** (1971) 127.
[23] A. M. Shams El-Din, *Electrochim. Acta* **7** (1962) 285.
[24] R. Littlewood and E. J. Argent, *ibid.* **4** (1961) 114.
[25] J. O'M. Bockris, *J. Chem. Phys.* **24** (1956) 817.
[26] P. Delahay, 'New Instrumental Methods in Electrochemistry', Interscience, New York (1954) p. 32.